

Fault-Tolerant Operation of Multiphase Permanent-Magnet Machines Using Iterative Learning Control

Ali Mohammadpour, *Student Member, IEEE*, Sandipan Mishra,
and Leila Parsa, *Senior Member, IEEE*

Abstract—Fault-tolerant control (FTC) techniques for multiphase permanent magnet (PM) motors are usually designed to achieve maximum ripple-free torque under fault conditions with minimum ohmic losses. A widely accepted approach is based on flux distribution or back EMF (BEM) model of the machine to calculate healthy phase currents. This is essentially an open-loop technique where currents are determined (based on motor fault models) for each fault scenario. Therefore, it is highly model dependent. Since torque pulsation due to open-circuit faults and short-circuit faults are periodic, learning and repetitive control algorithms are excellent choices to minimize torque ripple. In this paper, iterative learning control (ILC) is applied as a current control technique for recovering performance in multiphase PM motor drives under fault conditions. The ILC-based FTC needs torque measurement or estimation, but avoids the need for complicated fault detection and fault diagnosis algorithms. Furthermore, BEM-based FTC and ILC-based FTC are proposed that initiates the learning from a model-based approximate guess (from the BEM method). Therefore, this method combines the advantages of both model information as well as robustness to model uncertainty through learning. Hence, the proposed method is well suited for high-performance safety critical applications. Finite element analysis and experimental results on a five-phase PM machine are presented for verification of the proposed control schemes.

Index Terms—Fault-tolerant control, five-phase machines, iterative learning control, permanent-magnet machine.

I. INTRODUCTION

THERE is an increasing interest to move toward more electric drive systems in various applications. Although design requirements are varying, there is no room to make a compromise on safety and reliability of the electric drive in aerospace and naval systems. In the aerospace industry, failure of an actuator, which in worst case scenario will result in loss

Manuscript received August 29, 2013; revised November 17, 2013; accepted December 10, 2013. Date of publication December 20, 2013; date of current version April 4, 2014. This work was supported by the Office of Naval Research under Award N000140910886. Recommended for publication by Associate Editor E. Levi.

A. Mohammadpour and L. Parsa are with the Department of Electrical, Computer and Systems Engineering, Rensselaer Polytechnic Institute, Troy, NY 12180 USA (e-mail: mohama3@rpi.edu; parsa@ecse.rpi.edu).

S. Mishra is with the Department of Mechanical, Aerospace and Nuclear Engineering, Rensselaer Polytechnic Institute, Troy, NY 12180 USA (e-mail: mishrs2@rpi.edu).

Color versions of one or more of the figures in this paper are available online at <http://ieeexplore.ieee.org>.

Digital Object Identifier 10.1109/JESTPE.2013.2295537

of the aircraft, must have a probability of $<1 \times 10^{-9}$ per flight hour. Faults in motor windings and converter switches have probability of 1.4×10^{-8} and 8.6×10^{-5} , respectively [1]. Thus, safe fail approach for fault tolerance is not a valid option in safety-critical applications. In other words, the drive system has to continue operation with acceptable performance even under such fault conditions.

Extensive research work has been reported on fault-tolerant operation of conventional three-phase motor drives under fault conditions [2], [3]. Five-phase machines are advantageous over conventional three-phase machines for fault-tolerant operation. In five-phase machines, when faults occur in one or more of the phases, the machines can still continue operation using the remaining healthy phases without additional hardware [4], [5]. Several research works have been reported over the last decade on back EMF model (BEM)-based fault-tolerant control (FTC) of permanent magnet (PM) machines. Fault-tolerant operation of the multiphase PM machines and the multiphase induction machines are discussed in [6] and [7], respectively.

However, these works consider only sinusoidal distribution of stator windings. A current control strategy for a five-phase PM motor is introduced in [8], where combined first- and third-harmonic order currents are used for the excitation of the healthy stator phases. This method does not minimize the stator ohmic loss and output torque ripple. Wang *et al.* [9] describes an optimal torque control strategy for fault-tolerant PM brushless ac drives, which enables ripple-free torque operation while minimizing the copper loss under voltage and current constraints. In [10], an optimal control technique for the fault-tolerant operations of the multiphase PM machines is proposed where currents in the healthy phases are controlled to continue the machine operation with minimum stator ohmic loss and minimum output torque ripple constraints. An FTC technique for five-phase PM motors with trapezoidal BEM is presented in [11] where fundamental and third-harmonic current components are used for the excitation of the healthy stator phases.

Most of the fault-tolerant schemes are based on flux density and BEM model of the multiphase machine. They just consider torque ripple resulting from interaction between supplied currents and BEM. Furthermore, cogging torque, high frequency flux and BEM harmonics, and current measurement

errors are usually ignored. Since under fault condition there is a periodicity in the electromagnetic torque of multiphase PM machines, repetitive [12], [13] and learning [14]-based approaches are attractive candidates to operate drive system with minimum torque ripple. Repetitive control is preferred in systems with continuous operation, while iterative learning control (ILC) is the preferred algorithm for run-to-run control. However, since the model of the motor does not involve any dynamics (i.e., we ignore transients), both repetitive control and ILC reduce to the same algorithm.

We will address the ILC design problem in this paper (which is equivalent to the repetitive control problem). The ILC [15] is a feedforward control design technique for repetitive processes. The ILC algorithms use information from earlier trials (executions or experimental runs) of the repetitive process to improve the performance in the current trial. The key design issue in the ILC is the efficient utilization of this information to improve the performance of the closed-loop system using as few trials as possible. Due to its simple design, analysis, and implementation, ILC has been employed in many applications including industrial robotics [16], [17], computer numerical control tools [18], injection molding systems [19], rapid thermal processing [20], and microscale robotic deposition [14]. A review of ILC can be found in [21]. In [22], an ILC algorithm was employed to minimize torque ripple of a three-phase PM synchronous motor where cogging torque, flux harmonics, and current sensing errors are analyzed as pulsating torque ripple sources. Since the torque ripple due to open-circuit and short-circuit faults is also repetitive with a known period, related to operating speed, ILC is a natural choice for ripple minimization under fault conditions.

In this paper, we propose ILC as an efficient technique to improve fault tolerance of multiphase PM machines. Three FTC schemes will be discussed in this paper for multiphase PM machines. First, we review BEM-based FTC schemes. The BEM-based FTC scheme performance is greatly dependent on BEM data and fault information. Furthermore, it is really challenging to consider the effect of cogging torque and current measurement errors.

Therefore, an ILC-based control is introduced for improved fault tolerance as second scheme. The ILC-based scheme offers a torque ripple-free solution with approximate information of the BEM waveform, without using any explicit fault information. As an added benefit, with ILC-based FTC scheme, repeating torque disturbances at the pulsating frequencies are also compensated. This ripple-free operation of PM machine using proposed ILC-based approach requires measurement or estimation of motor output torque. In addition, because there is no fault information in ILC-based scheme, the initial learning starts from healthy operation currents and learning is executed to reject torque ripple without considering total ohmic loss of the machine.

Thus, finally third scheme proposed here is a combined FTC that inherits benefits of both BEM-based FTC and ILC-based FTC (BEM+ILC). This scheme is a promising control technique for multiphase PM motor drives to ensure high performance under fault conditions. This FTC scheme offers guaranteed ripple-free operation with optimal currents that

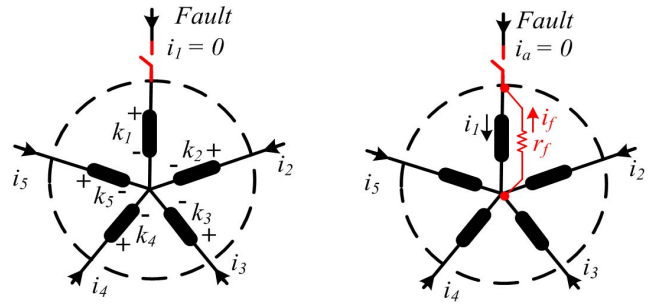


Fig. 1. Faults in a five-phase machine, from left to right: open-circuit fault and short-circuit fault.

minimize total ohmic losses of the PM machine. Finite element analysis (FEA) results are presented for a five-phase PM machine to investigate proposed control schemes. It should be noted that although focus of this paper is on single-phase faults in a conventional star-connected five-phase PM machine, proposed control techniques can be extended to multiphase PM machines with any number of phases and any connection of stator windings under open-circuit and short-circuit faults. The proposed control techniques are developed assuming constant speed reference and constant load torque. There is no limit for operation under variable load torque as long as system is able to follow reference current profiles. For continuously changing speed, the proposed algorithm will need to be modified to depend on position rather than time-based learning.

This paper is organized as follows. Section II reviews BEM-based FTC for multiphase PM machine drives. The ILC-based FTC scheme is introduced in Section III. Verification of proposed control technique by FEA and experimental tests are presented in Sections IV and V, respectively. Finally, conclusions are drawn in Section VI.

II. BEM-BASED FTC

In this section, BEM-based FTC scheme is briefly reviewed for multiphase PM machines. Schematic view of open-circuit fault and short-circuit fault in one phase of a five-phase motor is shown in Fig. 1. It is assumed that the faulty phase will be disconnected from external supply under short-circuit fault condition.

An optimal open-circuit fault technique for five-phase PM machines was proposed in [10] and [23] considering all possible connections of stator windings as well as fault types. Current control problem was posed as an optimization problem, where the optimization objective is to produce ripple-free electromagnetic torque with minimum ohmic losses under open-circuit fault conditions. A simple closed-form equation was used to calculate reference optimal currents in all cases where a lookup table is utilized to represent the effect of fault type. Assuming constant speed operation, the phase current vector, i , and speed-normalized BEM vector, k , of an n -phase motor are defined as

$$\begin{aligned} i &= [i_1 \ i_2 \ \dots \ i_n]^T \in \mathfrak{R}^n \\ k &= [k_1 \ k_2 \ \dots \ k_n]^T \in \mathfrak{R}^n. \end{aligned} \quad (1)$$

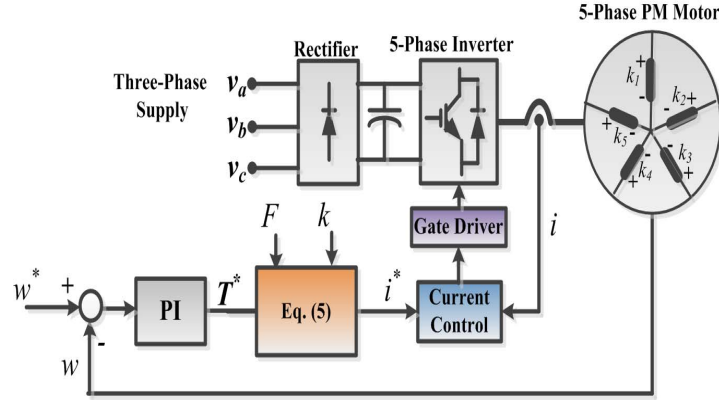


Fig. 2. Block diagram of BEM-based FTC scheme.

Elements of BEM vector k are time varying scalars that form an n -phase balanced set and their instantaneous values depend on electromagnetic design of the motor and rotating speed. The goal of the open-circuit FTC is to achieve desired ripple-free torque with minimum ohmic loss

$$i^* = \arg \min_i \frac{1}{2} i^T i. \quad (2)$$

Subject to

$$\begin{aligned} F^T i &= 0 \\ k^T i &= T^* \end{aligned} \quad (3)$$

where T^* is desired torque. Matrix F is fault matrix and its elements are selected to represent constraints imposed by stator winding connection and fault location(s).

Thus, the objective function for this purpose is defined as

$$f(p_1, p_2, i) = \frac{1}{2} i^T i + p_1 (T^* - k^T i) + p_2 F^T i \quad (4)$$

where p_1 and p_2 are Lagrangian multipliers. The optimization problem can be solved analytically offline to find the optimal currents as

$$i^* = \frac{F' k}{k^T F' k} T^* \quad (5)$$

where F_l^{-1} is left inverse of matrix F defined as

$$F_l^{-1} = (F^T F)^{-1} F^T \quad (6)$$

and F' is given by

$$F' = (I_n - F F_l^{-1}). \quad (7)$$

Using this method, fault-tolerant operation of a five-phase PM motor under open-circuit faults is possible. However, successful operation of fault-tolerant scheme depends on BEM model of the motor and relatively complicated fault detection.

Using a similar approach, short-circuit fault tolerant under steady-state operation is analyzed in [24]. It was assumed that fault current is limited to nominal current of the motor and mutual coupling between phases is negligible. Optimization

problem can be solved to find the optimal currents for short-circuit faults as

$$i_{\text{ref}} = \frac{T_{\text{ref}}}{k^T F' k} F' k + \frac{k^T F_r^{-T} i_{\text{sc}}}{k^T F' k} F' k - F_r^{-T} i_{\text{sc}} \quad (8)$$

where F_r^{-T} is right inverse of matrix F^T , defined as

$$F_r^{-T} = F (F^T F)^{-1} \quad (9)$$

and F' is given by (7). i_{sc} is equal to zero for healthy operation and for a single-phase fault is given by

$$i_{\text{sc}} = \begin{bmatrix} i_f \\ 0 \end{bmatrix}. \quad (10)$$

Fault current will depend on operating conditions specifically motor speed and fault impedance. Therefore, for the most common case of short-circuit fault with zero fault impedance, short-circuit current can be calculated through analytical equations, FEA, or experimental tests. However, in practice short-circuit faults occur through a resistive path with unknown value of resistance value. Furthermore, estimation of fault current and its effect on output torque of the motor is quite complicated.

Fig. 2 shows a conceptual block diagram of BEM-based FTC. Reference speed and measured speed are represented by w^* and w , respectively. Proper operation of the BEM-based FTC depends on accuracy of the machine model and a relatively complicated fault detection and fault diagnosis algorithm. Complete instructions to set F for multiphase motors together with a comprehensive lookup table for five-phase motors are presented in [10]. A current controller is used to generate gate drive signals for the voltage source inverter and to make the stator phase currents to follow the optimal current references. Short-circuit faults represent more challenging scenario because current of faulty phase depends on fault resistance. A detailed mathematical representation of optimal solution for short-circuit faults is explained in [24]. As it can be seen from (8), optimal currents under short-circuit fault are even more tied with operating condition of the motor including short-circuit current of faulty phase. Current of the faulty phase on the other hand is dependent on working speed and fault impedance. Thus, in Section III, a learning-based approach is

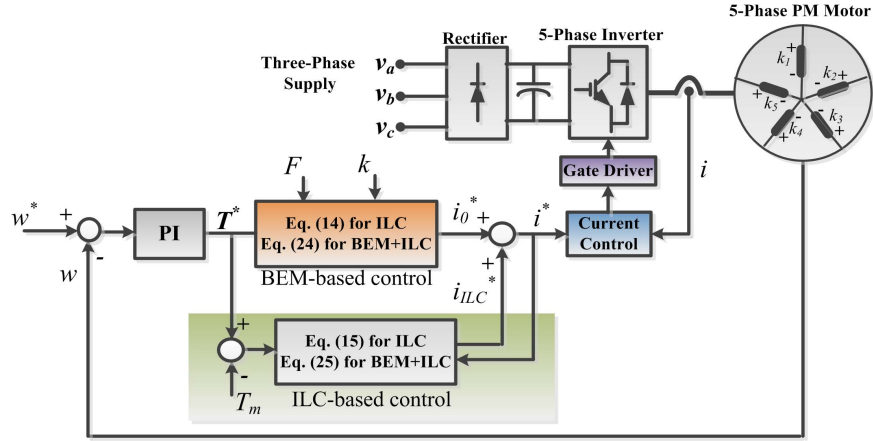


Fig. 3. Block diagram of the ILC-based and BEM+ILC-based FTC schemes.

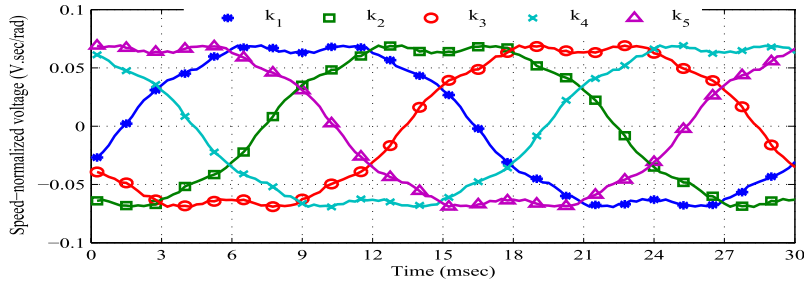


Fig. 4. Speed-normalized BEM waveform of the five-phase PM machine.

proposed to decrease or even eliminate dependency on BEM model and fault conditions.

III. ILC-BASED FTC

The ILC is based on the fact that the performance of a system that executes the same task multiple times can be improved by learning from previous executions. For a PM machine under fault condition, periodic torque ripple is generated during each line cycle. This torque ripple can be minimized by updating healthy phase currents, in each line cycle, considering torque ripple characteristic and input current of previous line cycle. A brief review is presented here. Application of ILC for fault tolerance in multiphase motors was proposed in [25]. Open-circuit faults were studied for a five-phase PM motor using FEA. Here, we will consider both open-circuit fault and short-circuit fault. Furthermore, experimental test results are provided to investigate effectiveness of proposed control techniques.

A. ILC-FTC

Consider the discrete time, linear time invariant, single-input single-output system

$$y_j(m) = P(q)u_j(m) + d(m) \quad (11)$$

where m is the time index, j is the iteration index, q is the forward time-shift operator $qx(m) \equiv x(m+1)$, y_j is the output, u_j is the control input, and d is an exogenous signal that repeats each iteration.

Here, y is the output torque T_m , u is vector of reference input current i^* , and d is any repeating term of torque like oscillating torque due to fault or cogging torque. $P(q)$ is BEM vector of the PM machine. Therefore, plant equation is given by

$$T_m = k^T i + T_d \quad (12)$$

where T_d is oscillating torque disturbance. The performance or error signal is defined by $e_j(m) = y_d(m) - y_j(m)$ where y_d is the desired output. A typically used linear ILC learning algorithm is

$$u_{j+1}(m) = Q(q)[u_j(m) + L(q)e_j(m+1)] \quad (13)$$

where $Q(q)$ and $L(q)$ are defined as the Q -filter and learning function, respectively.

Fig. 3 shows block diagram of the proposed ILC-based FTC scheme. Motor output torque, T_m , is measured and compared with the reference torque, T^* . Torque error and reference current of the current iteration (j) are used to calculate reference current of the next iteration. Therefore, torque measurement is required in ILC-based FTC. In addition, the ILC-based FTC tries to minimize torque ripple regardless of fault condition. As a result, it can react to a fault without the need for a complicated fault detection and diagnosis algorithm, and at the same time eliminates any repetitive torque ripple due to model mismatches.

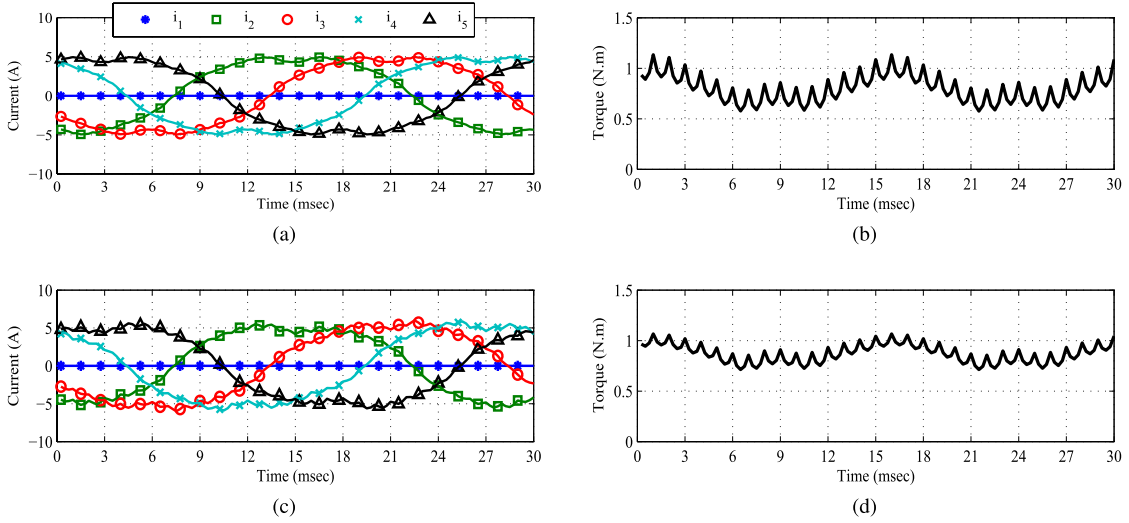


Fig. 5. FEA results for input currents and output torque with ILC-based FTC scheme. (a) and (b) Iteration 0. (c) and (d) Iteration 1.

Assuming a balanced five-phase BEM for PM machine, reference currents can be found using

$$i_0^* = ((k^T k)^{-1}) T^* k. \quad (14)$$

Note that k is position dependent (and hence time dependent), as shown in Fig. 4. There is no need to have an exact model of the BEM waveform of the machine because learning-based controller updates currents in each iteration in order to minimize torque error. The objective of learning is to minimize torque error, $T^* - T_m$. Thus, the update law for the ILC current $i_{ILC,j+1}$ is given by

$$i_{ILC,j+1}^* = i_{ILC,j}^* + \beta k (k^T k)^{-1} e_j \quad \text{for } j \geq 0 \quad (15)$$

where

$$e_j = T^* - T_{m,j}. \quad (16)$$

Learning function is selected using (14) considering the fact that we want to calculate updated currents for new iteration from torque error. Here, convergence of the proposed ILC-based FTC is analyzed. Output torque of the motor at iteration $j + 1$ is given by

$$T_{m,j+1} = k^T i_{j+1}^* + T_d. \quad (17)$$

Note that the objective of ILC is to make i_{j+1}^* converge to the ideal reference current i^* such that $T_{m,j+1}$ tends to T^* .

Theorem: The learning scheme (15) is convergent by choosing β to satisfy $0 < \beta < 2$.

Proof: Torque error at iteration $j + 1$ is calculated as

$$\begin{aligned} e_{j+1} &= T^* - T_{m,j+1} = k^T i^* - k^T i_{j+1}^* \\ &= k^T [i^* - i_{ILC,j}^* - \beta k (k^T k)^{-1} e_j] \\ &= e_j - \beta k^T k (k^T k)^{-1} e_j. \end{aligned} \quad (18)$$

This can be simplified as

$$e_{j+1} = (1 - \beta) e_j. \quad (19)$$

It is easy to see that the convergence condition is $|1 - \beta| < 1$, which can be expressed as $0 < \beta < 2$.

Therefore, tracking error will converge to zero with proper selection of β . However, it should be noted that in the experimental tests, learning scheme was modified slightly to enhance its robustness against perturbations and nonperiodic disturbances. The modified equations of motor model and learning scheme are given as

$$\begin{aligned} T_{m,j+1} &= k^T i_{j+1}^* + T_d + T_{d,j+1} \quad (20) \\ i_{ILC,j+1}^* &= (1 - \alpha) i_{ILC,j}^* + \beta k (k^T k)^{-1} e_j \\ &\quad + \gamma k (k^T k)^{-1} e_{j+1} \quad \text{for } j \geq 0 \quad (21) \end{aligned}$$

where $T_{d,j+1}$ is nonrepeating torque disturbance. Selection of α and γ values is a tradeoff between perfect learning and robustness. With these new definitions, tracking error is calculated similarly to be equal to

$$e_{j+1} = \frac{1 - \alpha - \beta}{1 + \gamma} e_j + \frac{\alpha k^T i_0^* - T_{d,j+1}}{1 + \gamma}. \quad (22)$$

Thus, the convergence condition is given by

$$\left| \frac{1 - \alpha - \beta}{1 + \gamma} \right| < 1. \quad (23)$$

It is worth to note that in the presence of nonperiodic torque term $T_{d,j+1}$ and forgetting factor α , the tracking error will not converge to zero, but its upper bound is limited.

Although ILC-based FTC operation is possible without fault information, solutions found by this method are not necessarily optimal from ohmic loss point of view. Therefore, in Section III-B, ILC-based FTC is combined with BEM-based FTC to utilize advantages of both methods for a high-performance motor drive in safety critical applications.

B. BEM+ILC-FTC

An FTC method is proposed in this section that combines model-based and ILC methods. Fig. 3 shows the block diagram of the BEM+ILC-based FTC scheme. As noted in earlier ILC literature, initialization of the ILC scheme is critical to guarantee rapid convergence. We therefore propose using the

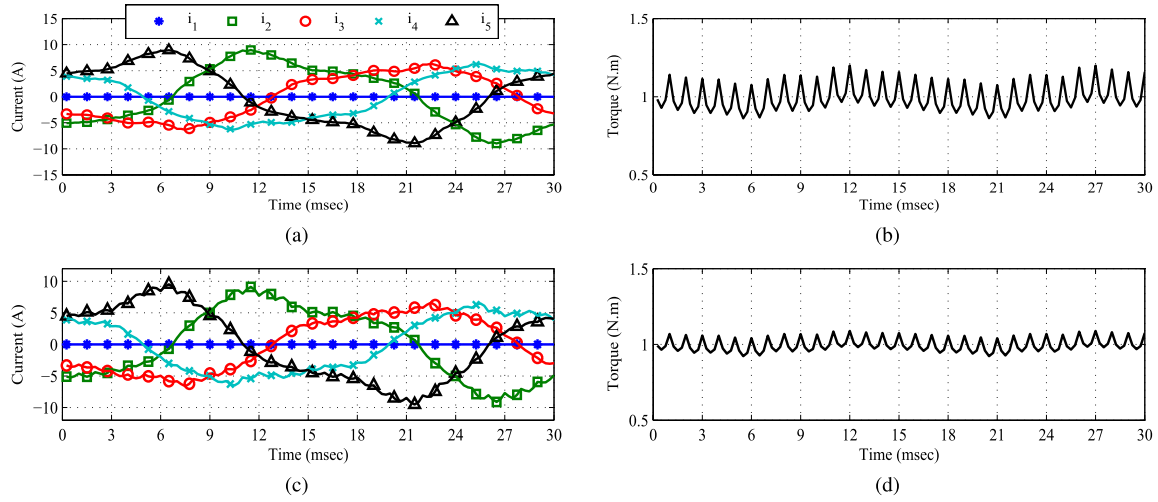


Fig. 6. FEA results for input currents and output torque with BEM+ILC-based FTC scheme. (a) and (b) Iteration 0. (c) and (d) Iteration 1.

initial solution under fault condition from the BEM-based FTC scheme to initialize the learning algorithm

$$i_0^* = (F'k(k^T F'k)^{-1})T^*. \quad (24)$$

Assuming exact BEM data and fault information, initial solution of the BEM+ILC method is exactly the same as BEM-FTC solution and will provide ripple-free torque with minimum ohmic losses. With BEM+ILC method, initial solution of BEM method will be adjusted precisely using ILC to ensure ripple-free torque. Hence, with BEM+ILC method, ripple-free torque is achieved with a five-phase current set very close to analytical solution obtained by BEM-FTC method that minimizes ohmic losses.

Fault-tolerant currents are updated using the following equation:

$$i_{ILC,j+1}^* = i_{ILC,j}^* + \beta (F'k(k^T F'k)^{-1}) (T^* - T_{m,j}) \quad \text{for } j \geq 0 \quad (25)$$

where learning function is selected based on the solution for BEM-based control method. The BEM+ILC-based control scheme can be seen as two control algorithms running in parallel to ensure high performance operation of multiphase PM machines under fault conditions. Even in the case of failure of one algorithm, due to faults in torque transducer or wrong fault detection, the other algorithm can offer high level of fault tolerance. Convergence analysis of BEM+ILC method is similar to the analysis discussed for ILC method in Section III-B. The FEA results of a five-phase PM machine are presented in Section IV to analyze three FTC schemes discussed in Sections III-A and B.

IV. FEA OF PROPOSED FTC SCHEMES

In order to evaluate ILC-based FTC schemes, 2-D FEA results are presented in this section for a five-phase PM machine. The FEA is widely accepted method for design and analysis of electric machines [26]. The FEA is used to solve partial differential equations of the electromagnetic fields in the electric motor for analyzing and simulating the

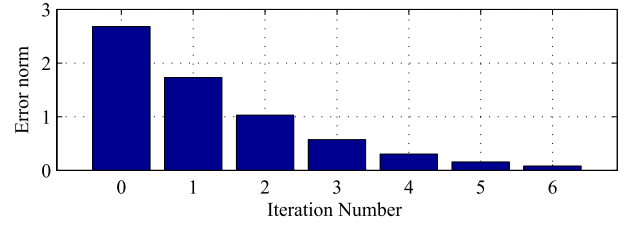


Fig. 7. Two-norm of torque error versus iteration number for ILC-based FTC scheme.

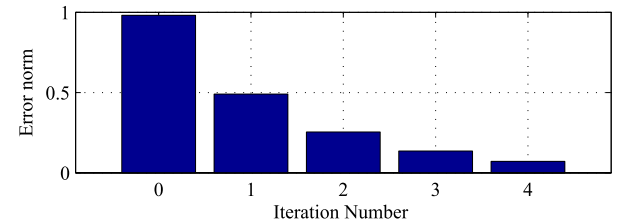


Fig. 8. Two-norm of torque error versus iteration number for BEM+ILC-based FTC scheme.

behavior of nonideal motors. Under fault conditions, BEM-based control will bring system close to its optimal operating point from ohmic loss point of view with minimum torque ripple. The ILC-based controller on the other hand will adjust currents around optimal operating point to achieve ripple-free torque. Therefore, the BEM+ILC-based control has benefits of both control methods. However, BEM model of the machine, fault detection and diagnosis, and torque information are required for this method. It should be noted that a rough model of the machine BEM is enough for successful operation of the BEM+ILC-based FTC.

A five-phase four-pole PM machine is considered in this paper. The stator of the machine has 15 slots with double-layer windings. The inner diameter of the stator, the outer diameter of stator, and the stack length of the machine are 65, 120, and 80 mm, respectively. The air-gap length of the machine is 0.5 mm. The PMs are NdFeBr with residual flux density, $B_r = 1.2$ T. The speed-normalized BEM waveform is

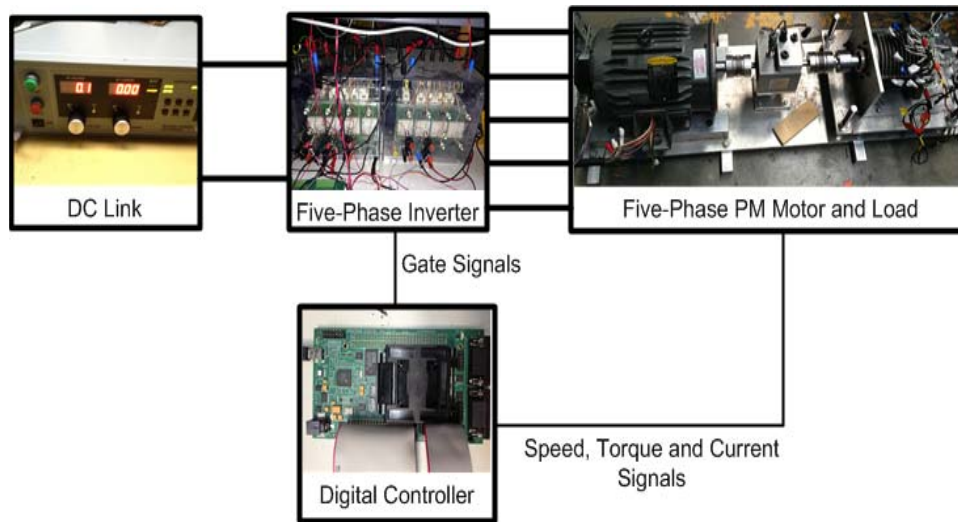


Fig. 9. Five-phase motor drive system used for experimental tests.

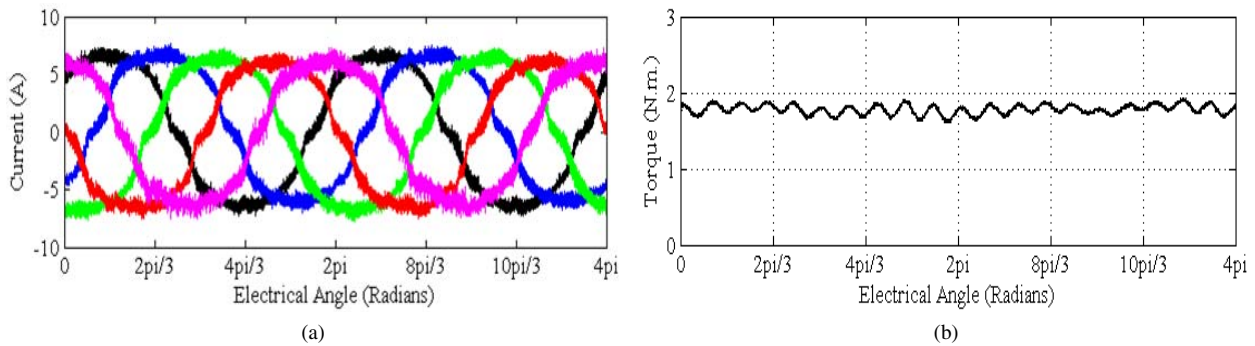


Fig. 10. Five-phase current and output torque under normal operation.

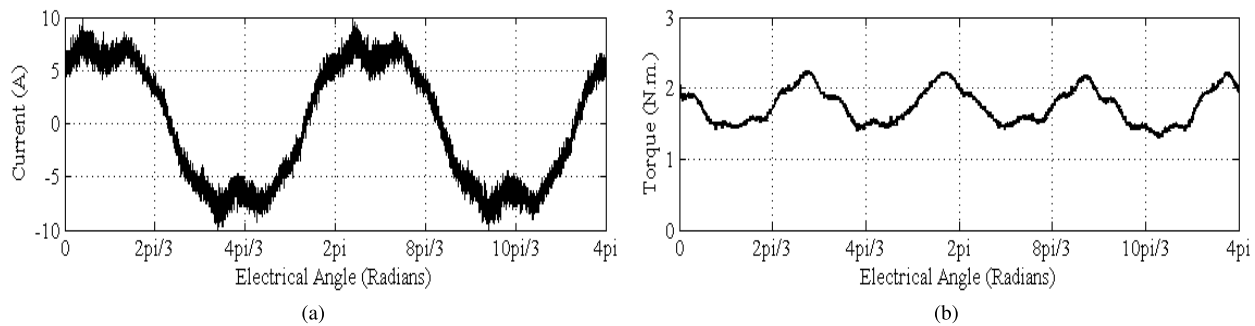


Fig. 11. Current of faulty phase and output torque under short-circuit fault condition.

shown in Fig. 4. The fast Fourier transform of the measured BEM data is carried out to obtain its frequency components. It is found that the machine BEM contains 11% third harmonic and 3% seventh harmonic. The BEM data are used to calculate optimal currents using FTC schemes developed in the previous sections under different fault conditions. The FEA results are presented here assuming single-phase open-circuit fault condition on a star-connected machine. The FEA results for ILC-based FTC scheme are shown in Fig. 5. It is important to note that no fault information is used in the ILC-based FTC. Therefore, initial solution is healthy operation solution as

in (14). Fig. 5(a) and (b) show input currents and output torque of the machine before initiating ILC, respectively. Phase 1 is assumed to be faulty phase. It is obvious that output torque ripple is very large. There are two major ripple components of output torque. First ripple component with higher frequency and smaller magnitude is due to cogging torque. Second ripple component has higher magnitude and lower frequency and it is introduced here due to open-circuit fault of phase 1. The input current and output torque information are used in learning, (25), to calculate input currents for the first iteration as shown in Fig. 5(c). Output torque of the

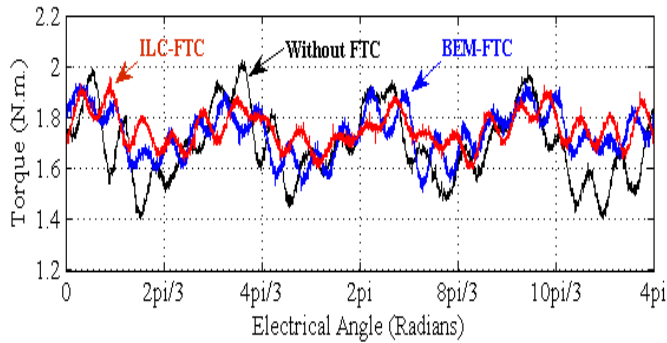


Fig. 12. Output torque under open-circuit fault condition.

machine for first iteration is shown in Fig. 5(d). Although torque ripple is still large for a high performance system, but there is significant reduction in torque ripple.

Simulation results for BEM+ILC-based FTC scheme are shown in Fig. 6. Here, fault information is used for initial solution as in (24). Fig. 6(a) and (b) show input currents and output torque of the machine before initiating ILC, respectively. Phase 1 is again assumed to be faulty phase. It can be seen that with BEM+ILC-based FTC scheme torque ripple of initial solution is significantly smaller than initial solution of ILC-based FTC. The torque ripple in this case is mainly due to cogging and fault effect is compensated by BEM-based FTC used for initial solution. The ILC is used to cancel torque ripple and achieve a ripple-free torque. Input current and output torque data are used in learning, (25), to calculate input currents for first iteration as shown in Fig. 6(c). The output torque of the machine for first iteration is shown in Fig. 6(d). The two-norm of torque error is used to evaluate the operation of learning quantitatively. Fig. 7 shows two-norm of torque error for six iterations with ILC-based FTC scheme. The two-norm of the torque error for BEM+ILC-based control scheme is also shown in Fig. 8. It can be seen that two-norm of torque error is decreasing significantly at each new iteration. The BEM+ILC-based control scheme converges faster than ILC-based control scheme because of better initial solution.

V. EXPERIMENTAL RESULT

To verify the proposed control strategy by experiments, five-phase four-pole PM machine of previous section is considered in this paper. Experimental test results under both open-circuit fault and short-circuit fault are presented.

The block diagram of the drive system to implement the proposed fault-tolerant technique is shown in Fig. 3. A 256-pulse/revolution optical encoder is used to sense the rotor position angle. Motor speed is compared with the reference speed to obtain the speed error. A PI controller is used to estimate reference torque, which decides the amplitudes of the reference current profiles. Using the fault information, appropriate fault matrix is selected for the normal or fault-tolerant operation of the motor under BEM-based FTC technique. Five-phase PM machine in this paper has a trapezoidal BEM waveform that can be estimated with sinusoidal functions of fundamental and third-harmonic frequencies of angular

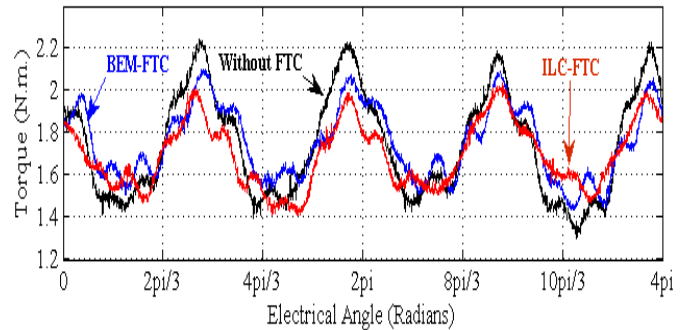


Fig. 13. Output torque under short-circuit fault condition.

velocity. Therefore, BEM waveform is estimated based on instantaneous rotor position acquired by the encoder.

Well known five-phase to dq transformation together with PI controllers and space vector pulsewidth modulation (SVPWM) are used for current control. The SVPWM-based vector control is selected due to its excellent performance in normal operation.

Fig. 9 shows the five-phase PM motor drive used for experimental tests. An insulated-gate bipolar-transistor-based five-leg two-level voltage source inverter is used as the motor drive for the experimental verification of the proposed solutions. The line currents are sensed with four Hall effect current sensors. A digital controller is used for the implementation of the control scheme. Proposed ILC-based approach is implemented along with standard vector control and additional computational burden due to ILC is not significant. In addition, using proposed control approach, one may even skip complicated fault identification scheme. Additional memory is required in order to save input current and torque error information of each line period (iteration). However, considering continuing progress in microcontrollers used in high-performance motor control applications, the additional computational and memory burden of the proposed control algorithm are not really significant. The machine is tested with a reference speed of 600 r/min. Load torque under the normal operating condition is ~ 1.7 Nm. For ILC-based control, output torque of the motor is estimated using simple BEM model of the motor where cogging torque is neglected. This estimation technique is simple and effective. Furthermore, this makes ILC more interesting for practical application by eliminating the need for an expensive torque transducer. Fig. 10 shows steady state currents [Fig. 10(a)] and output torque [Fig. 10(b)] waveform of the motor under normal operation. It can be seen that currents are just proportional to their corresponding phase BEMs. Output torque shows a small ripple due to cogging torque, which is not considered in optimal current calculations. It should be noted that experimental test results for output torque are obtained using a torque transducer with a bandwidth of 200 Hz.

The PM machine used in this paper has a very large short-circuit current at 600 r/min. Therefore, short-circuit tests are carried out using a 0.5- Ω auxiliary fault resistor to prevent damage to the motor windings and to avoid possible demagnetization of PMs. When fault occurs in one of the phases of the motor, output torque shows oscillating behavior.

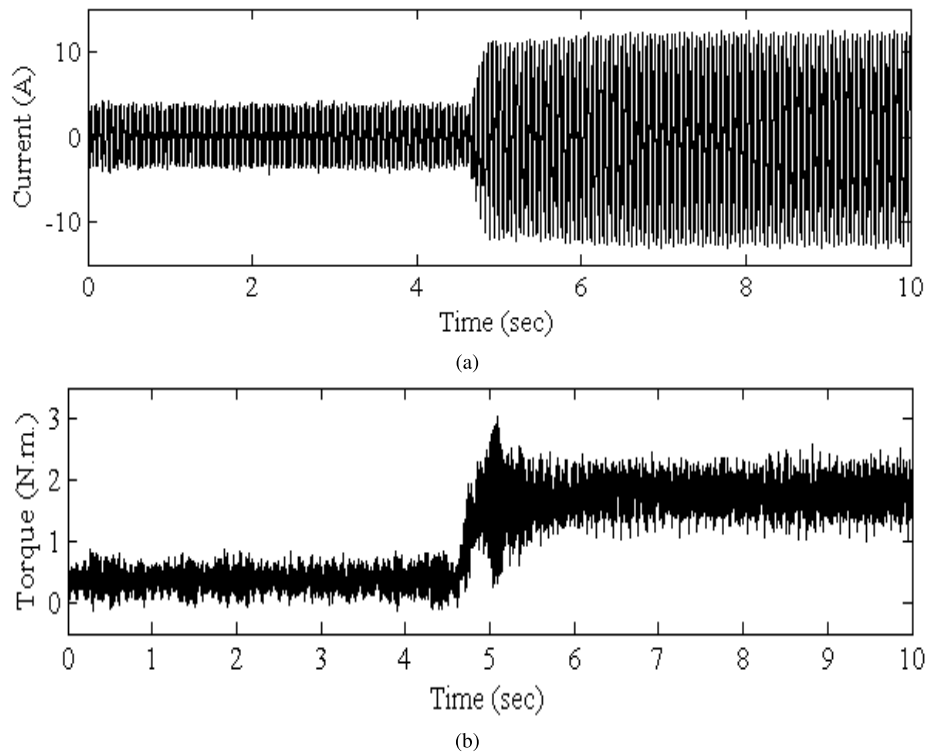


Fig. 14. Experimental results for step change in load torque under star connection and single-phase open-circuit fault condition. (a) Current in a healthy phase. (b) Output torque.

For example, current of the faulty phase and output torque of the motor are shown in Fig. 11(a) and Fig. 11(b) under short-circuit fault condition. As expected fault current waveform is similar to that of the motor BEM. It can be seen that short-circuit current results in large oscillations in the output torque, which in turn can cause mechanical vibration of the motor and acoustic noise. The experimental results of the output torque for the same load torque are shown in Figs. 12 and 13 for open-circuit fault and short-circuit fault, respectively. Results are presented for three test cases: 1) without using FTC; 2) using BEM-FTC; and 3) finally, ILC-FTC. It can be seen that using FTC, either ILC or BEM, torque ripple is reduced compared with non-FTC operation. Output torque measurement for BEM+ILC-based control is not shown in this graph as it gives almost the same result as BEM-based FTC. This can be justified by the fact that torque estimation method used here considers torque ripple component due to fault condition. It can be seen that for both fault types, FTC techniques offer significantly smaller torque ripple compared with the operation without using FTC. Furthermore, ILC-based FTC shows slightly smaller torque ripple than BEM-based FTC. For instance, under open-circuit fault condition (Fig. 12) torque ripple without using FTC is $\sim 35\%$. With BEM-FTC and ILC-FTC torque ripple is $\sim 22\%$ and 18% , respectively. For short-circuit fault condition, torque ripple is 56% without FTC as shown in Fig. 13. Torque ripple is decreased to 38% using BEM-FTC and 32% using ILC-FTC. Finally, it should be noted that minimization of torque ripple is related to the performance of the current controller in addition to proper calculation of reference currents. This is why torque ripple

seems to be still relatively large in spite of application of proposed FTC techniques. However, it should be mentioned that ILC is a plug-in control and is fairly decoupled from the main control (hysteresis, vector, and so on). Although hysteresis-based control usually has better performance in terms of torque ripple, but its not desirable control technique for high performance multiphase drives due to problems associated with variable switching frequency.

In order to investigate dynamic performance of the proposed control technique under steady-state fault conditions, experimental tests were executed under an abrupt change in load torque. Fig. 14 shows current of a healthy phase and output torque of the motor under a step change in load torque. It can be seen that drive system shows good dynamic performance even under steady-state fault condition.

Finally, experimental tests are carried out to analyze transition from healthy to faulty operation using proposed control approach. Fig. 15 shows test results during transition from healthy operation to single-phase open-circuit fault condition. Load torque and motor reference speed are the same for healthy and faulty operation. As it can be seen from Fig. 15(a), current of faulty phase drops to zero as a result of open-circuit fault. Currents of two healthy phases, adjacent to faulty phase [Fig. 15(b)] and nonadjacent to faulty phase [Fig. 15(c)] are also shown before and after fault. It can be seen that there is relatively big increase in the current of adjacent healthy phase. Last waveform in Fig. 15(d) shows output torque of the motor. Although torque ripple is higher under steady-state postfault operation, transition from normal to faulty operation is smooth.

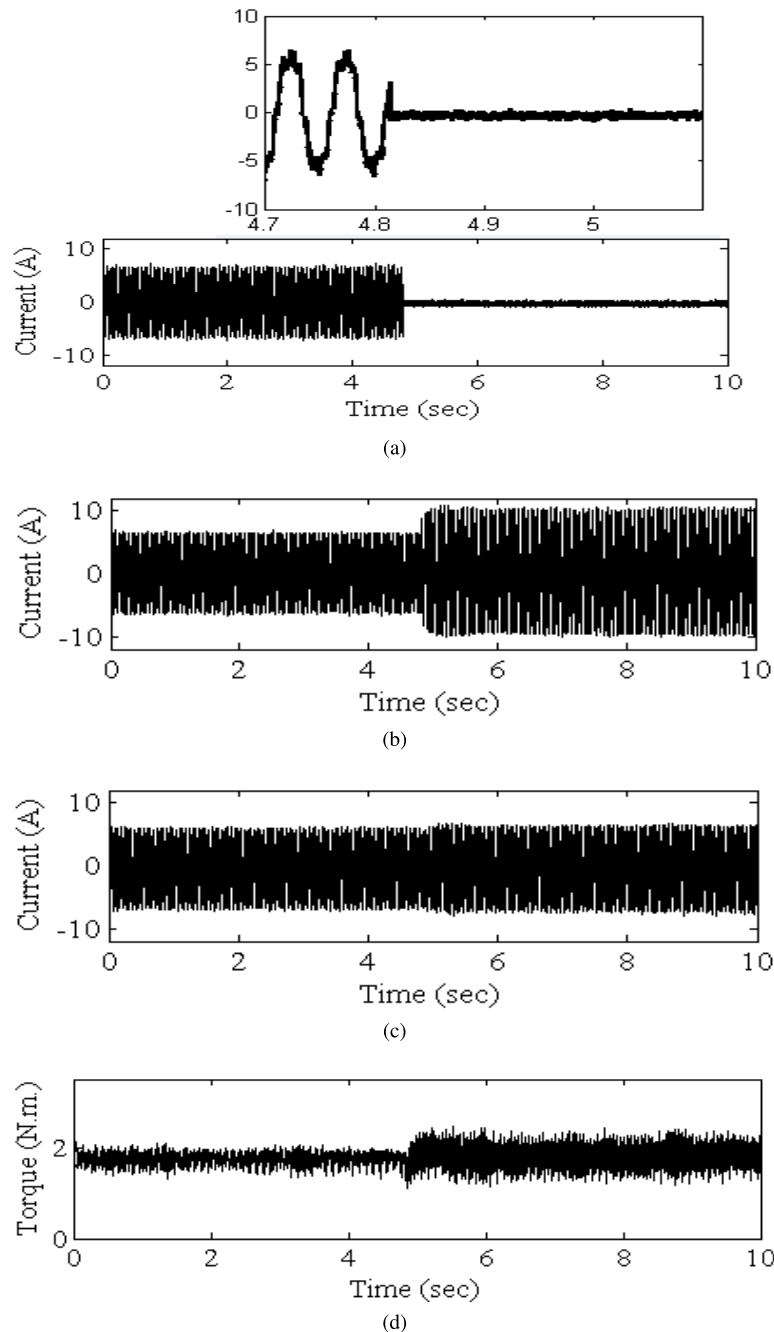


Fig. 15. Experimental results for transition from healthy condition to single-phase open-circuit fault condition. (a) Current of faulty phase. (b) Current of adjacent healthy phase. (c) Current of nonadjacent healthy phase. (d) Output torque.

VI. CONCLUSION

A new approach based on ILC is proposed to improve performance of multiphase PM machines under open-circuit and short-circuit fault conditions. The BEM-based control technique minimizes torque ripple and copper loss using fault information. Different from BEM-based FTC scheme, ILC-based FTC scheme does not need fault information. However, solutions obtained by ILC-based control are not necessarily optimal from ohmic loss point of view. The BEM+ILC-based control scheme offers ripple-free output torque after couple of iterations, while currents are optimized to minimize total ohmic losses of the machine. In fact ILC can

be used as a parallel control algorithm with BEM-based FTC to ensure high-performance operation of the fault-tolerant PM machine.

REFERENCES

- [1] W. Cao, B. Mecrow, G. Atkinson, J. Bennett, and D. Atkinson, "Overview of electric motor technologies used for more electric aircraft (MEA)," *IEEE Trans. Ind. Electron.*, vol. 59, no. 9, pp. 3523–3531, Sep. 2012.
- [2] R. Errabelli and P. Mutschler, "Fault tolerant voltage source inverter for permanent magnet drives," *IEEE Trans. Power Electron.*, vol. 27, no. 2, pp. 500–508, Feb. 2012.
- [3] A. Sayed-Ahmed, B. Mirafzal, and N. Demerdash, "Fault-tolerant technique for delta-connected AC-motor drives," *IEEE Trans. Energy Convers.*, vol. 26, no. 2, pp. 646–653, Jun. 2011.

- [4] A. Abd Hafez, R. Todd, A. Forsyth, and A. Cross, "Direct current ripple compensation for multi-phase fault-tolerant machines," *IET Electr. Power Appl.*, vol. 5, no. 1, pp. 28–36, Jan. 2011.
- [5] A. El-Refai, "Fault-tolerant permanent magnet machines: A review," *IET Electr. Power Appl.*, vol. 5, no. 1, pp. 59–74, Jan. 2011.
- [6] A. Mohammadpour, A. Gandhi, and L. Parsa, "Design and control of fault-tolerant permanent magnet machines," in *Proc. IEEE WEMDCD*, Mar. 2013, pp. 108–116.
- [7] J.-R. Fu and T. Lipo, "Disturbance-free operation of a multiphase current-regulated motor drive with an opened phase," *IEEE Trans. Ind. Appl.*, vol. 30, no. 5, pp. 1267–1274, Sep./Oct. 1994.
- [8] N. Bianchi, S. Bolognani, and M. Pre, "Strategies for the fault-tolerant current control of a five-phase permanent-magnet motor," *IEEE Trans. Ind. Appl.*, vol. 43, no. 4, pp. 960–970, Jul./Aug. 2007.
- [9] J. Wang, K. Atallah, and D. Howe, "Optimal torque control of fault-tolerant permanent magnet brushless machines," *IEEE Trans. Magn.*, vol. 39, no. 5, pp. 2962–2964, Sep. 2003.
- [10] A. Mohammadpour, S. Sadeghi, and L. Parsa, "A generalized fault-tolerant control strategy for five-phase PM motor drives considering star, pentagon, and pentacle connections of stator windings," *IEEE Trans. Ind. Electron.*, vol. 61, no. 1, pp. 63–75, Jan. 2014.
- [11] A. Mohammadpour and L. Parsa, "A unified fault-tolerant current control approach for five-phase PM motors with trapezoidal back EMF under different stator winding connections," *IEEE Trans. Power Electron.*, vol. 28, no. 7, pp. 3517–3527, Jul. 2013.
- [12] S. Hara, Y. Yamamoto, T. Omata, and M. Nakano, "Repetitive control system: A new type servo system for periodic exogenous signals," *IEEE Trans. Autom. Control*, vol. 33, no. 7, pp. 659–668, Jul. 1988.
- [13] J. Ghosh and B. Paden, "Nonlinear repetitive control," *IEEE Trans. Autom. Control*, vol. 45, no. 5, pp. 949–954, May 2000.
- [14] D. Bristow and A. Alleyne, "A high precision motion control system with application to microscale robotic deposition," *IEEE Trans. Control Syst. Technol.*, vol. 26, no. 3, pp. 96–114, Jun. 2006.
- [15] S. Arimoto, S. Kawamura, and F. Miyazaki, "Bettering operation of robots by learning," *J. Robot. Syst.*, vol. 1, no. 2, pp. 123–140, 1984.
- [16] S. K. Tso and X. Ma, "Discrete learning control for robots: Strategy, convergence and robustness," *Int. J. Control*, vol. 57, no. 2, pp. 273–291, 1993.
- [17] K. Moore, M. Dahleh, and S. Bhattacharyya, "Learning control for robotics," in *Proc. Int. Conf. Commun. Control*, Oct. 1988, pp. 976–987.
- [18] D.-I. Kim and S. Kim, "An iterative learning control method with application for CNC machine tools," *IEEE Trans. Ind. Appl.*, vol. 32, no. 1, pp. 66–72, Jan./Feb. 1996.
- [19] H. Havlicsek and A. Alleyne, "Nonlinear control of an electro-hydraulic injection molding machine via iterative adaptive learning," *IEEE/ASME Trans. Mechatron.*, vol. 4, no. 3, pp. 312–323, Sep. 1999.
- [20] Y. Chen, J.-X. Xu, T. H. Lee, and S. Yamamoto, "An iterative learning control in rapid thermal processing," in *Proc. IASTED*, Aug. 1997, pp. 189–192.
- [21] D. Bristow, M. Tharayil, and A. Alleyne, "A survey of iterative learning control," *IEEE Control Syst. Mag.*, vol. 26, no. 3, pp. 96–114, Jun. 2006.
- [22] W. Qian, S. Panda, and J.-X. Xu, "Torque ripple minimization in PM synchronous motors using iterative learning control," *IEEE Trans. Power Electron.*, vol. 19, no. 2, pp. 272–279, Mar. 2004.
- [23] A. Mohammadpour, S. Sadeghi, and L. Parsa, "Fault-tolerant control of five-phase PM machines with pentagon connection of stator windings under open-circuit faults," in *Proc. 27th Annu. IEEE APEC Exposit.*, Feb. 2012, pp. 1667–1672.
- [24] A. Mohammadpour and L. Parsa, "Post-fault control technique for multi-phase PM motor drives under short-circuit faults," in *Proc. 28th Annu. IEEE APEC Exposit.*, Mar. 2013, pp. 817–822.
- [25] A. Mohammadpour, S. Mishra, and L. Parsa, "Iterative learning control for fault-tolerance in multi-phase permanent-magnet machines," in *Proc. ACC*, Jun. 2013, pp. 129–135.
- [26] N. Bianchi and S. Bolognani, "Design techniques for reducing the cogging torque in surface-mounted PM motors," *IEEE Trans. Ind. Appl.*, vol. 38, no. 5, pp. 1259–1265, Sep./Oct. 2002.



Ali Mohammadpour (S'08) received the B.S. degree from the University of Tabriz, Tabriz, Iran, in 2007, and the M.S. degree from the Sharif University of Technology, Tehran, Iran, in 2009, both in electrical engineering. He is currently pursuing the Ph.D. degree in electrical engineering with the Rensselaer Polytechnic Institute, Troy, NY, USA.

He was a Power Electronics Engineer in the industry from 2009 to 2010. He is the author of more than 15 papers in peer-reviewed journals and conference proceedings. He is an invited reviewer of major

journals and conferences. His current research interests include fault-tolerant motor drives, power electronic systems, and converters.



Sandipan Mishra received the B.Tech. degree from IIT Madras, Chennai, India, in 2002, and the Ph.D. degree from the University of California, Berkeley, CA, USA, in 2008, both in mechanical engineering.

He was a Post-Doctoral Researcher with the University of Illinois at Urbana-Champaign, Urbana, IL, USA, from 2008 to 2010. Since 2010, he has been with the Faculty Member of the Mechanical, Aerospace, and Nuclear Engineering Department, Rensselaer Polytechnic Institute, Troy, NY, USA.

His current research interests include systems and control, and precision mechatronics, as applied to advanced manufacturing, smart building systems, and adaptive optics.

Dr. Mishra is a recipient of the National Science Foundation Early CAREER Award in 2013 for control of additive manufacturing. He is a member of the American Society of Mechanical Engineers and the American Society of Plumbing Engineers.



Leila Parsa (S'00–M'05–SM'10) received the Ph.D. degree in electrical engineering from Texas A&M University, College Station, TX, USA.

She joined the Department of Electrical, Computer, and Systems Engineering, Rensselaer Polytechnic Institute, Troy, NY, USA, in 2005, where she is currently an Associate Professor. Her current research interests include design, analysis and control of electromechanical energy converters and power electronics converters for various applications.

Dr. Parsa was a recipient of the 2010 RPI School of Engineering Research Excellence Award, the 2009 Office of Naval Research Young Investigator Award, the 2007 IEEE Industry Applications Society Outstanding Young Member Award, and the 2006 IEEE Industry Applications Society Transactions Paper Award.